Mineralogy and *in situ* S and Pb isotope characteristics of ore minerals from polymetallic mineralization in the Gierczyn-Przecznica area, SW Poland

Krzysztof FOLTYN[1, *], Gabriela A. KOZUB-BUDZYŃ[1], Yann LAHAYE[2], Adam PIESTRZYŃSKI[1], Paulina SKIRAK[1], Władysław ZYGO[1] and Jadwiga PIECZONKA[1]

[1] AGH University of Science and Technology, Al. Mickiewicza 30, 30-059 Kraków, Poland; ORCID: 0000-0002-5262-4136 [K.F.], 0000-0002-3489-9822 [G.K.-B.], 0000-0001-6649-6772 [A.P.], 0000-0003-3223-5982 [P.S.], 0000-0001-8124-1209 [W.Z.], 0000-0002-3525-0996 [J.P.]

[2] Geological Survey of Finland, Vuorimiehentie 2K 02150 Espoo, Finland, ORCID: 0000-0002-3982-4854

Chlorite-mica-quartz schist in the Gierczyn-Przecznica area in SW Poland contains polymetallic ores which were the source of tin and cobalt in the past. This mineralogical study revealed the presence of silver-bearing minerals including members of the tetrahedrite (Ag <3 apfu) and freibergite series (3 < Ag < 8 apfu), galena (0.26–1.48 wt.% Ag), and a phase with the chemical composition of Te-rich canfieldite $Ag_8Sn(S,Te)_6$. In Przecznica Sn-sulphides are represented by stannite while cobaltite is the most abundant host for cobalt, followed by Co-bearing arsenopyrite. Glaucodot, ullmannite and members of the löllingite-rammelsbergite solid-solution series $(Fe,Ni,Co)As_2$ also contain cobalt but are scarce in the samples. An exposure in the "Psi Grzbiet" area is characterized by the presence of Ag, Ni, Sb and Te minerals accompanied by very small amounts of As-bearing phases (represented by arsenopyrite) while the mineralogical composition in the Przecznica area is characterized by an abundance of As phases and a lack of Sb minerals. Sulphur isotopes of sulphides from Przecznica are heavier than in most deposits related to the Karkonosze Granite intrusion, while their Pb isotope signature in galena suggests an Early Paleozoic pre-Variscan affinity rather than a Variscan one.

Key words: Pb isotopes, S isotopes, polymetallic mineralization, cobalt, Sudetes Mts.

INTRODUCTION

Mineral deposits often include a complex assemblage of elements and with the increasing demand for high-technology metals (for example cobalt, indium, gallium, tellurium), and with improvement in ore processing technology, increasing attention is being given to potential by-products. The "metal wheel" (Verhoef et al., 2004) shows the link between main products and by-products, but in some cases, mineralization might include elements with contrasting geochemical characteristics. One such example is the Stara Kamienica Schist Belt in SW Poland, where tin and cobalt, elements not often found together, were mined in the past in the Gierczyn-Przecznica area. The tin ores were mainly exploited from the 16th to 18th century, while cobalt was mined in the 18th and 19th century when the maximum annual production reached 2200 tons of ore

(Michniewicz et al., 2006). The 1930s and 1940s were times of renewed interested in these deposits and subsequently detailed geological investigation was made in the 1950s and 1960s with exploration based on the existing mining works and borehole cores (Madziarz and Sztuk, 2008). Mining has not been resumed and the resources are considered subeconomic but prognostic and perspective tin resources in the whole area of the Stara Kamienica Schist Belt are estimated at ~25 Mt of ore and 100 kt of metallic tin (Mikulski and Małek, 2020). The origin of this deposit is still not fully understood, with genetic models ranging from syngenetic-sedimentary, epigenetic-hydrothermal to stratiform exhalative-volcanogenic (Speczik and Wiszniewska, 1984; Michniewicz et al., 2006; Mochnacka et al., 2015). The geological unit hosting the polymetallic mineralization had a complicated evolution and its untangling can provide a new insight into the formation of tin and cobalt deposits in metamorphosed terranes. This study provides new data on the origin and chronology of the mineralization as well as on the mineralogical characterization of semi-massive sulphide samples from old dumps in Przecznica and newly found sulphide assemblages from a mica schist with boudin-like quartz lenses exposed in the vicinity of the "Psi Grzbiet" mine. Particular attention was given to mineral phases containing elements of inter-

* Corresponding author, e-mail: kfoltyn@agh.edu.pl

est such as Co, Ni, Sn, Te and Ag, which might constitute a valuable by-product and affect the present sub economic status of the deposit.

GEOLOGICAL SETTING

The Karkonosze-Izera Massif (KIM) is located in the south--central part of the West Sudetes on the NE margin of the Bohemian Massif, at the border of Poland and the Czech Republic (Fig. 1). The KIM can be subdivided into the Karkonosze Granite intrusion and its metamorphic envelope. The granite bodies crystallized around 312–306.9 Ma and are considered to be postcollisional, transitional between I-, and S-type, mostly peraluminous, strongly evolved and fractionated (Mikulski, 2007; Mikulski et al., 2020). The Strzegom-Sobótka Pluton comprises four varieties of granite, formed in the following succession: a two-mica granite crystallized at 304.8 Ma, followed by a biotite granodiorite and hornblende-biotite granite at 301.9–297.1 Ma and finally with a biotite granodiorite at 294.4 Ma (Turniak et al., 2014).

The metamorphic envelope of the Karkonosze Granite Pluton encompasses four structural units of Neoproterozoic-Paleozoic age: the Izera-Kowary Unit (IKU, the Early Paleozoic continental crust of the Saxothuringian Basin), the Ještěd Unit (the Middle Devonian to Lower Visean sedimentary succession deposited on the NE passive margin of the Saxothuringian Terrane), the Southern Karkonosze Unit (metamorphosed sediment and volcanic rocks filling the Saxothuringian Basin) and the Leszczyniec Unit (an Early Ordovician obducted fragment of the Saxothuringian Basin sea floor) (Mazur and Kryza, 1996; Mazur and Aleksandrowski, 2001; Mochnacka et al., 2015). The Izera-Kowary Unit, separated by the Late Carboniferous

Karkonosze Pluton into northern and southern parts, consists of gneisses and mica schists. The northern Izera Massif part includes the texturally diverse Izera Gneisses, its structural development was completed during Late Devonian to Early Carboniferous deformation of the Early Paleozoic porphyritic Izera and Rumburk granites (Borkowska et al., 1980; Oberc-Dziedzic et al., 2005). The evolution of the Karkonosze-Izera Massif involved two major stages. The first was a compressional event with overthrusting, predated by HP/LT metamorphism of the South Karkonosze and Leszczyniec units, while the second stage is an extensional event linked with the collapse of the orogen and intrusion of the Karkonosze Granite (Mazur and Kryza, 1996; Mazur and Aleksandrowski, 2001). The Izera-Kowary Unit also contains several E–W trending metasedimentary belts which are composed of mica schists with minor interbeds of amphibolite, calc-silicate rocks, quartzite and quartz-feldspar schist, all metamorphosed under conditions of upper greenschist and lower amphibolite facies (Żelaźniewicz et al., 2003). The Stara Kamienica Schist Belt, dipping toward the north at angles of 37.5–57.5 , hosts low-grade cassiterite mineralization disseminated in chlorite-mica-quartz schist (in some cases also rich in almandine garnet), forming a stratabound body and locally accompanied by a polymetallic sulphide/sulphosalt association with a dominance of chalcopyrite and pyrrhotite (Piestrzyński and Mochnacka, 2003; Michniewicz et al., 2006; Mochnacka et al., 2015 and references therein). Tin concentration increases in the middle part of the schist sequence and is sandwiched between the main gneiss member in the north and the intra-schist gneiss member in the south (Michniewicz et al., 2006). The tin-bearing schists are 100–200 m thick and surrounded by barren schist, the distinction between them being based on geochemical data (Sn content >0.004%) rather than on lithological boundaries (Michniewicz et al., 2006).
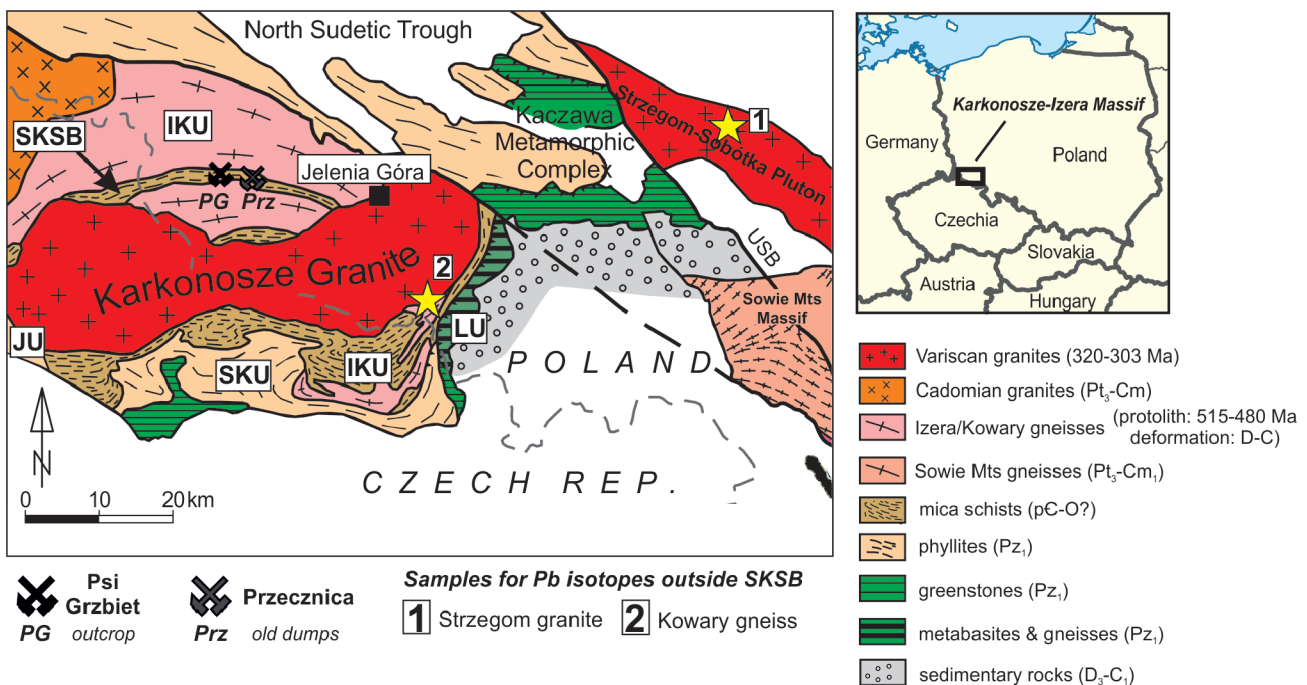

Fig. 1. Geological map of the Karkonosze-Izera Massif and adjacent geological units (modified from Mazur et al., 2010)

SKSB – Stara Kamienica Schist Belt, IKU – Izera-Kowary Unit, JU – Ještěd Unit, SKU – Southern Karkonosze Unit,
LU – Leszczyniec Unit, USB – Sudetic Boundary Fault

Two types of cassiterite have been distinguished in the area, "brown" and "colourless". Cassiterite is locally accompanied by an assemblage of sulphides, comprising mainly pyrrhotite, chalcopyrite, sphalerite, arsenopyrite, native bismuth, galena and pyrite. Another kind of pyrrhotite-dominated mineralization with only traces of chalcopyrite and with no spatial correlation to tin horizons also occurs in the form of thin laminae, lenses and impregnations (Michniewicz et al., 2006).

It is inferred that the tin-polymetallic mineralization most likely originated from a complex interplay of hydrothermal, magmatic and metamorphic processes (Małek and Mikulski, 2021), but the details are still a matter of discussion and several genetic models have been suggested (see Michniewicz et al., 2006; Mochnacka et al., 2015). The most widely accepted proposals involve hydrothermal activity related to granitic intrusion with some authors attributing it to the Cambrian-Ordovician granitic protolith of the Izera Gneisses (pre-metamorphic, e.g., Michniewicz et al., 2006) and others to the Variscan Karkonosze Granite (post-metamorphic e.g., Mochnacka et al., 2015).

MATERIAL AND METHODS

In contrast to cassiterite, the white transparent crystals of which provide a challenge for macroscopic identification in a typical mica-quartz-chlorite-garnet assemblage (Fig. 2A–B),

the polymetallic sulphide mineralization can be easily identified. Samples were collected from exposure and old dumps north of Kotlina village (50°55'43.1"N, 15°23'11.8"E), in the area of an old "Psi Grzbiet" ("Hundsrücken" in German, meaning Dog's Ridge or Dog's Back) mine near Gierczyn. A few metres NE from the former Hundsrücken shaft (adapted as the "Gierczyn" mine shaft no. 2), there is a small exposure where a forest trail was cut 1.5 m deep into the mica-chlorite schists. These rocks contain foliation-concordant quartz lenses, ranging from several mm in diameter, up to bigger boudin-like quartz masses up to 15 cm in diameter. Quartz is locally accompanied by disseminated sulphide accumulations, usually present at the contact of larger quartz lenses with mica schist or as individual veinlets in massive quartz (Figs. 2C, D and 3A, B). Research material from the old dumps in the area of St Maria-Anna (50°55'34.8"N, 15°26'13.3"E) in Przecznica is of disseminated to semi-massive sulphide mineralization in mica schists (Fig. 2E, F).

METHODS

Optical light microscopy was used to characterize the ore minerals and define textural relationships in 25 rock samples. Chemical analyses of sulphides, sulphosalts and tellurides in micro-area were carried out using a *JEOL JXA-8230 Super-Probe* electron microprobe at the Laboratory of Critical Elements, AGH-KGHM in Kraków. It was operated in the wave-
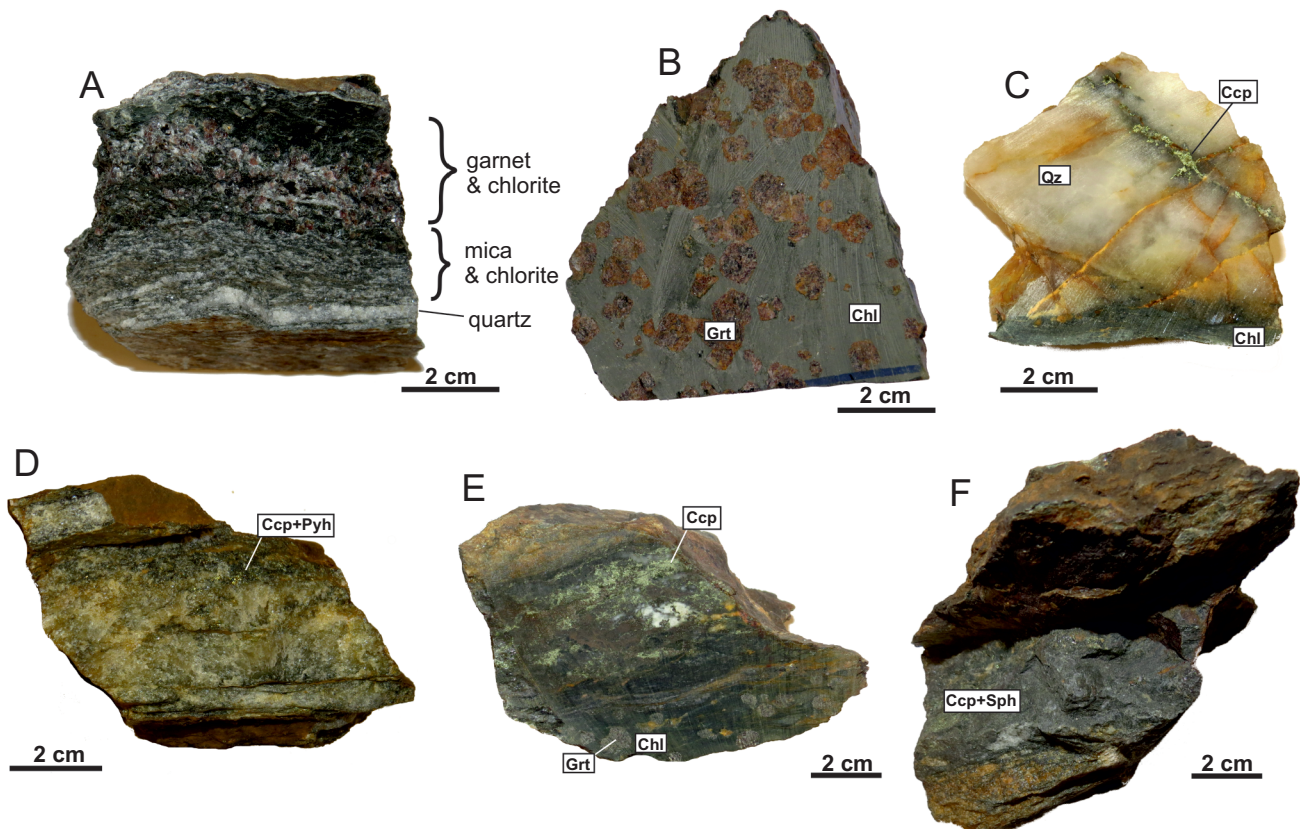
Fig. 2A –typical sample of mica-quartz-chlorite±garnet schist from the quarry in Krobica (~3.5 km west from Gierczyn); B – chlorite schist with exceptionally large garnet crystals (up to 1 cm in diameter) from Krobica; C – quartz lens in mica-chlorite schist containing a chalcopyrite veinlet from the "Psi Grzbiet" area; D – chalcopyrite-pyrrhotite disseminations in mica-quartz schist from the "Psi Grzbiet" area; E – semi-massive chalcopyrite in altered and deformed mica-quartz-chlorite-garnet schists from Przecznica; F – semi-massive chalcopyrite-sphalerite assemblage in mica-quartz-chlorite-garnet schist from Przecznica

Ccp – chalcopyrite, Chl – chlorite, Grt – garnet, Pyh – pyrrhotite, Qz – quartz, Sph – sphalerite.

length-dispersion mode at an accelerating voltage of 20 kV, a probe current of 20 nA for sulphide and 10 nA for sulphosalts. The following standards and spectral lines were used for sulphides and sulphosalts: FeS_2 (FeKα, SKα), chalcopyrite (CuKα), ZnS (ZnKα), Ag (AgLα), In_2Se_3 (InLα), stibnite (SbLα), Co (CoKα), CdS (CdLα) Bi_2S_3 (BiMα), galena (PbMα), Bi_2Te_3 (TeLα), GaAs (AsLα), Sb_2Se_3 (SeLα) and SnS (SnLα). Data were corrected to the ZAF procedure using *JEOL* software for electron microprobe.

Sulphur isotope analyses of pyrite and sphalerite were made using a *Nu Plasma HR multicollector ICPMS* at the Geological Survey of Finland in Espoo together with a *Photon Machine Analyte Excite* laser ablation system. Samples were ablated in He gas (gas flows = 0.4 and 0.1 l/min) within a HelEx ablation cell (Müller et al., 2009). S isotopes were analysed at medium resolution. During the ablation, the data were collected in static mode (^{32}S, ^{34}S). Single spot samples were ablated at a spatial resolution of 30 μm, using a fluency of 3.5 J/cm^2 and at 5 Hz on thin sections. The total S signal obtained was between 0.5 and 3.0 V. Under these conditions, an internal precision of ^{34}S/^{32}S $\leq \pm 0.000005$ (1 SE) is obtained after a 20 s baseline and 50–60 s of signal integration. One in-house pyrite standard was used for external standard bracketing (Py-1) whereas the pyrite standard PPP-1 (Gilbert et al., 2014) and in-house pyrite standard Py2 were used for quality control. The in-house pyrite standard Py-1 had been previously measured by gas mass spectrometry. For a $\delta^{34}S_{CDT}$(‰) reference value of –0.6 ±0.3‰ (1σ) we found an average value of –0.3 ±0.5‰ (1σ, n=7). The in-house pyrite standard Py2 was previously measured by gas mass spectrometry. For a $\delta^{34}S_{CDT}$(‰) reference value of –0.4 ±0.5‰ (1σ) we found an average value of 0.0 ±0.4‰ (1σ, n=7). One chalcopyrite (Cpy1) in-house standard was used as an external standard and a second in-house chalcopyrite standard Cpy2 was used for quality control. The in-house chalcopyrite standard Cpy2 had been previously measured by gas mass spectrometry. For a $\delta^{34}S_{CDT}$(‰) reference value of –0.7 ±0.5‰ (1σ) we found an average value of –0.6 ±0.3‰ (1σ, n=15).

Pb-Pb isotope analyses were performed using the same equipment as for the *in situ* sulphur isotope measurements. All analyses were made using rasters with a stage stepping speed of 1 μm/s. Ablation conditions were: 3 m beam diameter, 3 Hz pulse frequency, 3 J/cm^2 beam energy density. A single Pb-Pb measurement included a 1 minute baseline measurement (measure zero) prior to a batch of ratio measurements, each of the latter consisting of data acquisition for 45 s with laser on. The MC-ICP-MS is equipped with 9 Faraday detectors and amplifiers with 10^{11} Ω resistors. Baseline and ablation data were measured on the peak, collected in static mode (^{208}Pb, ^{207}Pb, ^{206}Pb, ^{204}Pb, ^{205}Tl, ^{203}Tl). The raw data were filtered at 2 s and corrected for mass discrimination using an exponential law. The mass discrimination factor for Pb was determined using a ~10 ppb Tl solution nebulized at the same time as the sample, using a desolvating nebulizer. A galena from Broken Hill was used to monitor the precision and accuracy of the measurements, every ten samples, over the whole period of analysis. The average accuracy obtained is estimated to be better than 1.7‰ (1σ) for ^{208}Pb/^{204}Pb, 2.1‰ (1σ) for ^{207}Pb/^{204}Pb, 2.2‰ (1σ) for ^{206}Pb/^{204}Pb and 0.1‰ (1σ) for ^{207}Pb/^{206}Pb, compared with the certified values of Stevenson and Martin (1986) and Townsend et al. (1998).

Application of *in situ* LA MC-ICP-MS eliminates the effect of potentially incomplete physical separation of galena from other sulphide minerals in bulk analytical methods, and therefore the lead isotope ratio in galena depends solely on the sources of

metals and the age of crystallization (Molnár et al., 2016, 2018). The samples analysed represent chlorite-quartz-mica schist-hosted galena in a pyrite-sphalerite-galena assemblage from Przecznica and galena crystals in a stilbite-epidote-feldspar pegmatite druse from the Strzegom Massif, representing Variscan mineralization. Pb-Pb isotope analyses of K-feldspars from the Kowary Gneisses, representing metamorphosed Late Cambrian/Early Ordovician granitoids, were unsuccessful due to a too low concentration of lead.

RESULTS AND DISCUSSION

MINERALOGY

"PSI GRZBIET" AREA

The sulphide assemblage found at the exposure near the old Gierczyn mine shaft no. 2 (former "Hundsrücken" mine) is dominated by chalcopyrite, forming irregular, disseminated grains of 0.1–5 mm size hosted by quartz lenses as well as mica schist. In some cases it is accompanied by Fe-rich sphalerite (Table 1 and Fig. 3C). The chalcopyrite hosts a variety of mineral inclusions, primarily Ag, Sb, Ni and Bi minerals (Tables 2, 3 and Fig. 3C, D).

Silver-bearing minerals found in the samples include members of the tetrahedrite (Ag < 3 apfu) and freibergite series (3 < Ag <8 apfu), galena (0.26–1.48 wt.% Ag), and a phase with a chemical composition of Te-rich canfieldite $Ag_8Sn(S,Te)_6$ (Tables 2, 3 and Fig. 3I). Various assemblages of Pb-Sb-Bi±Ag sulphosalts are present in the samples, including Bi-rich jamesonite with a chemical composition similar to specimens from Brezno–Hviezda in Slovakia (Pršek et al., 2008) and the Stan Terg deposit in Kosovo (Kołodziejczyk et al., 2017), but their precise identification is difficult as they often form intergrowths of fine lamellae consisting of different mineral phases (Fig. 3H). Tellurides are generally rare in this area. Only one grain of joseite-A $Bi_4(S,Te)_3$ intergrown with native Bi and pyrrhotite in chalcopyrite and one small grain of hedleyite Bi_7Te_3 next to cassiterite in a sulphide free sample (Table 2) have been observed. Among other identified phases are ullmannite NiSbS and garavellite $FeSbBiS_4$, present as small inclusions (20–200 um) in chalcopyrite (Fig. 3C). Native bismuth, Bi-rich jamesonite, galena, pyrrhotite and Bi oxides intergrowths form needle-like crystals (0.2–3 mm long) in quartz (Fig. 3A, B) and partly in chalcopyrite (Fig. 3C, D). Bismuth sulphosalts, base metal sulphides and tetrahedrite group minerals are often a result of hydrothermal activity related to intrusions (e.g., Mederski et al., 2021). Textures, the presence of bismuth oxides and disseminated native bismuth in the samples described here suggest they are rather a remnant of primary sulphosalt mineralization, affected by regional metamorphism.

The mineral composition of samples found in the "Psi Grzbiet" area is very similar to the Ag-Cu-Pb-Sb-Bi sulphosalt assemblage reported from the schist-hosted Jialong Cu-Sn deposit in China (Liu et al., 2018). This is one of several tin deposits in the Jiuwandashan-Yuanbaoshan region, but while many of them are spatially and temporally related to Neoproterozoic granitic intrusions (Chen et al., 2018; Yue et al., 2022), U-Pb dating of cassiterite from the Jialong deposit revealed it is linked to the 422–420 Ma old Sirong shear zone (Yue et al., 2022). Similarities in geological context allow us to speculate that tin mineralization in the Stara Kamienica Schist Belt might have an
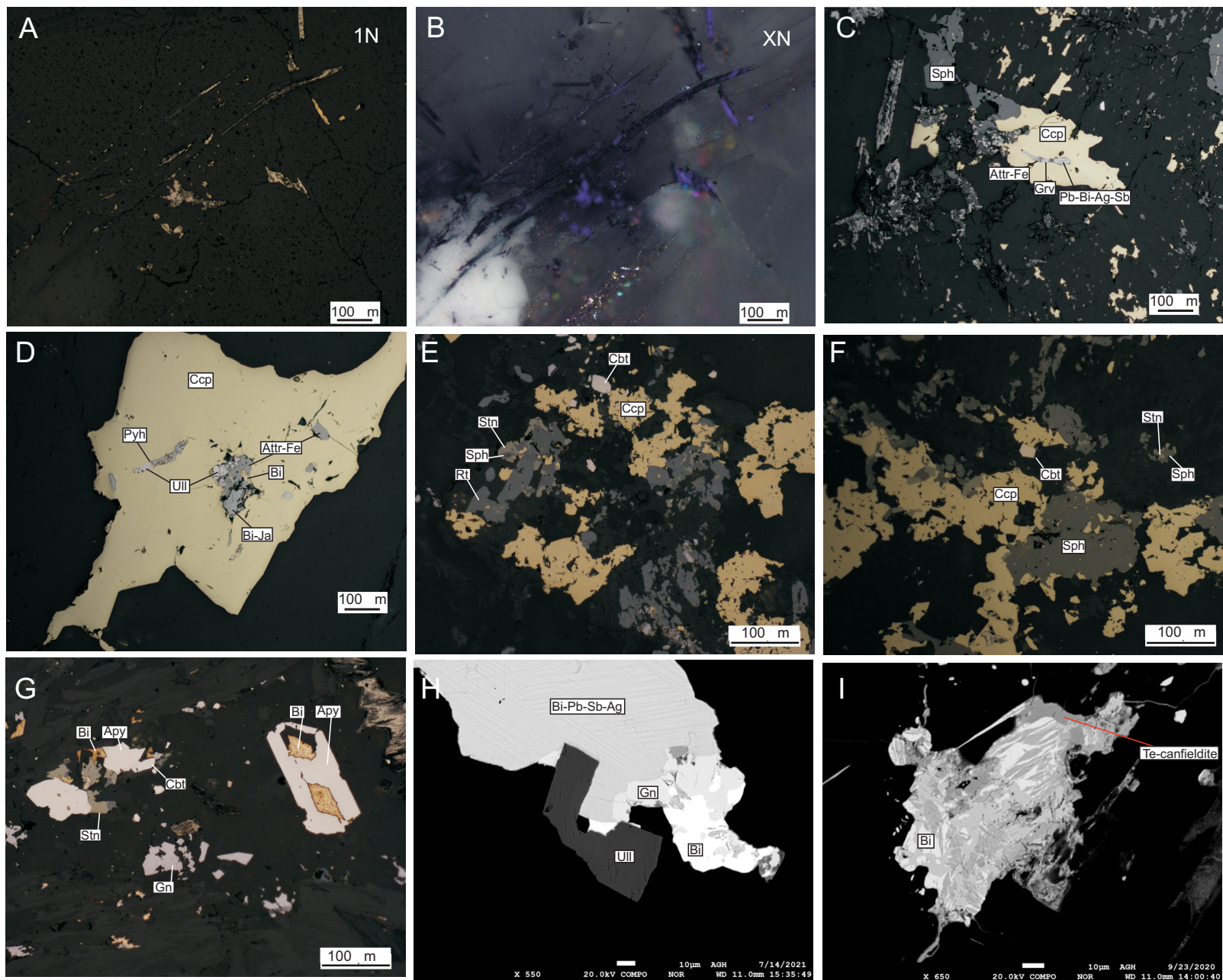
Fig. 3A–G – microphotographs of samples taken using a reflected light microscope; A, B – quartz-hosted needle-like crystals from the "Psi Grzbiet" area comprising a mixture of native bismuth, galena, pyrrhotite and Bi-rich jamesonite (A – plane polarized light; B – cross-polarized light); C – argentotetrahedrite-(Fe), garavellite and Pb-Bi-Ag-Sb sulphosalt hosted in chalcopyrite (the "Psi Grzbiet" area); needle-like crystals of sulphosalt replaced by a mixture of native bismuth, bismuth oxides and Bi-rich jamesonite on the left (the "Psi Grzbiet" area); D – argentotetrahedrite-(Fe), ullmannite, pyrrhotite, native bismuth and Bi-rich jamesonite assemblage in chalcopyrite (the "Psi Grzbiet" area); E, F – ore mineralization from Przecznica consisting of chalcopyrite, sphalerite, stannite, cobaltite and rutile; G – cobaltite-arsenopyrite intergrowth associated with stannite and native bismuth (Przecznica); H – BSE picture showing fine lamellae in a Bi-Pb-Sb-Ag sulphosalt associated with galena, native bismuth and ullmannite (the "Psi Grzbiet" area); I – BSE picture of Te-canfieldite adjacent to a mixture of native bismuth, galena and bismuth oxides (the "Psi Grzbiet" area)

Apy – arsenopyrite, Attr-Fe – argentotetrahedrite-(Fe), Bi – native bismuth, Bi-Ja – Bi-rich jamesonite, Ccp – chalcopyrite, Cbt – cobaltite, Gn – galena, Grv – garavellite, Pb-Bi-Ag-Sb – unidentified Pb-Bi-Ag-Sb sulphosalt, Pyh – pyrrhotite, Rt – rutile, Sph – sphalerite, Stn – stannite, Ull – ullmannite

Basic statistics of results of EPMA chemical analyses (in wt.%) of chalcopyrite and sphalerite from the "Psi Grzbiet" area and Przecznica

		S	Fe	Zn	Cu	Co	Sn	Ag	In	As	Se	Cd	Mn	Ge	Ga
Psi Grzbiet *Chalcopyrite* (n = 60)	Max	35.79	30.80	0.15	35.10	0.06	0.05	0.28	<0.02	<0.07	0.11	0.06	–	–	–
	Min	34.52	29.88	<0.03	33.35	0.02	<0.03	<0.02			<0.07	<0.02	–	–	–
	Mean	34.97	30.39	0.07	34.46	0.04	0.03	0.06				0.04	–	–	–
Przecznica *Chalcopyrite* (n = 26)	Max	35.10	30.56	0.31	35.34	0.06	0.08	0.14	<0.02	<0.06	0.10	0.06	–	–	–
	Min	33.49	29.49	<0.03	34.09	0.03	<0.03	<0.02			<0.07	<0.02	–	–	–
	Mean	34.31	30.13	0.12	34.94	0.05	0.04	0.05				0.04	–	–	–
Psi Grzbiet *Sphalerite* (n = 20)	Max	34.34	7.59	59.60	1.21	–	<0.02	<0.02	<0.02	0.06	–	1.41	0.03	<0.03	0.17
	Min	33.44	5.95	57.55	<0.03	–				<0.05	–	0.47	<0.02		<0.03
	Mean	33.94	6.74	58.81	0.31	–					–	0.85			
Przecznica *Sphalerite* (n = 33)	Max	34.60	9.68	59.89	0.56	0.07	<0.02	0.02	0.14	<0.04	–	0.47	0.04	0.03	<0.03
	Min	32.68	5.72	55.91	<0.03	<0.03		<0.02	<0.02		–	0.28	<0.02	<0.02	
	Mean	33.48	7.85	57.93	0.17	0.04			0.07		–	0.37			

– not measured

Results of EPMA chemical analyses (in wt.%) of sulphides, tellurides and sulphosalts from the "Psi Grzbiet" area

Mineral	S	Fe	Zn	Cu	Sb	Co	Sn	Ag	Ni	As	Se	Bi	Te	Pb	Sum
Arsenopyrite	21.04	34.87	<0.04	0.13	2.66	0.05	<0.02	<0.02	<0.02	40.54	<0.13	–	–	–	99.29
Arsenopyrite	18.86	33.26	<0.04	0.47	0.71	0.77	<0.02	<0.02	0.44	45.52	<0.13	–	–	–	100.03
Arsenopyrite	21.20	35.04	<0.04	<0.03	1.31	0.05	<0.02	<0.02	<0.02	41.58	<0.13	–	–	–	99.18
Arsenopyrite	20.54	35.20	<0.04	<0.03	3.06	<0.02	<0.02	<0.02	<0.02	40.89	<0.13	–	–	–	99.70
Arsenopyrite	19.13	27.10	0.09	0.26	0.92	6.95	<0.02	<0.02	0.73	45.28	<0.13	–	–	–	100.45
Arsenopyrite	19.53	24.93	<0.04	0.94	0.19	10.07	<0.02	<0.02	0.49	45.20	<0.13	–	–	–	101.35
Ullmannite	15.11	0.60	<0.04	<0.03	57.75	2.27	0.34	<0.02	25.08	0.27	0.12	–	–	–	101.50
Ullmannite	15.00	0.52	<0.04	<0.03	57.69	1.78	0.34	<0.02	25.57	0.24	0.01	–	–	–	101.14
Ullmannite	15.05	0.25	<0.04	<0.03	56.26	2.95	0.34	<0.02	24.48	0.12	0.09	–	–	–	99.52
Galena	12.99	0.28	<0.04	0.37	<0.03	–	–	1.48	–	<0.12	0.74	3.40	0.11	82.01	101.38
Galena	13.07	0.19	<0.04	0.26	<0.03	–	–	1.15	–	<0.12	0.84	3.56	0.10	81.69	100.86
Garavellite	25.28	11.41	0.37	0.95	27.89	–	–	<0.03	–	0.24	<0.12	35.21	<0.03	0.39	101.74
Native Bi	0.07	0.44	0.08	0.61	4.15	–	–	<0.03	–	<0.12	0.17	93.06	<0.03	<0.06	98.57
Native Bi	0.01	0.70	<0.04	1.24	3.15	–	–	<0.03	–	<0.12	<0.12	93.52	<0.03	<0.06	98.61
Joseite-A	5.00	0.60	<0.04	1.06	0.67	–	–	<0.03	–	0.18	2.61	78.14	10.93	0.68	99.86
Hedleyite	0.03	–	–	–	0.12	–	–	<0.03	–	–	0.70	79.07	19.50	<0.06	99.43
Te-canfieldite	9.51	<0.04	<0.04	<0.04	<0.03	–	8.12	62.09	–	<0.12	0.27	0.35	17.09	1.27	98.68
Te-canfieldite	9.80	<0.04	<0.04	<0.04	<0.03	–	7.67	61.07	–	<0.12	0.12	0.21	16.66	4.63	100.16
Bi-rich jamesonite	20.54	2.65	<0.04	0.51	25.11	–	–	<0.03	–	<0.12	<0.12	14.14	<0.03	37.63	100.59
Bi-rich jamesonite	20.20	2.78	<0.04	0.77	24.03	–	–	<0.03	–	<0.12	<0.12	15.14	<0.03	36.98	99.90
Bi-rich jamesonite	20.50	2.88	<0.04	0.63	25.79	–	–	<0.03	–	0.14	<0.12	12.41	<0.03	38.29	100.64
Bi-rich jamesonite	19.82	2.98	<0.04	0.73	24.65	–	–	<0.03	–	<0.12	<0.12	12.69	<0.03	39.05	99.92
Bi-Pb-Ag-Sb sulphosalt	17.47	0.67	<0.04	1.19	7.66	–	–	8.50	–	<0.12	0.36	41.79	0.08	23.35	101.08
Bi-Pb-Ag-Sb sulphosalt	17.25	0.12	1.44	0.09	5.59	–	–	8.58	–	<0.12	0.35	44.36	0.03	22.93	100.75
Bi-Pb-Sb-Ag sulphosalt	18.41	0.60	0.27	0.88	18.14	–	–	8.81	–	<0.12	0.23	28.53	<0.03	24.44	100.31

– not measured

Table 3

Representative results of EPMA chemical analyses (in wt.%) of members of the tetrahedrite [tetrahedrite-(Fe)] and freibergite series [argentotetrahedrite-(Fe)] from the "Psi Grzbiet" area

Mineral	Ag	S	Fe	Cu	Bi	Te	Pb	Sb	Zn	As	Se	Total
Argentotetrahedrite-(Fe)	34.21	20.77	5.83	14.16	0.09	<0.03	0.10	26.04	0.27	0.15	<0.13	101.62
Argentotetrahedrite-(Fe)	30.07	21.79	5.81	16.62	0.05	<0.03	<0.06	26.28	<0.05	<0.12	<0.13	100.62
Argentotetrahedrite-(Fe)	29.07	21.47	5.54	16.52	0.22	0.18	0.36	26.42	0.54	0.13	<0.13	100.43
Argentotetrahedrite-(Fe)	26.38	22.49	5.40	19.36	0.11	<0.03	0.09	26.96	0.64	0.16	0.14	101.71
Argentotetrahedrite-(Fe)	24.27	22.81	5.59	20.96	0.23	0.20	0.13	26.13	0.83	<0.12	<0.13	101.16
Argentotetrahedrite-(Fe)	22.48	22.87	5.62	22.15	0.17	0.11	0.08	26.53	0.98	0.14	<0.13	101.12
Argentotetrahedrite-(Fe)	20.59	23.36	5.59	23.26	0.32	0.12	0.13	27.11	0.93	0.16	<0.13	101.56
Argentotetrahedrite-(Fe)	20.20	23.05	5.58	23.32	0.46	<0.03	0.08	26.80	0.94	0.13	<0.13	100.57
Tetrahedrite-(Fe)	17.53	23.61	5.73	24.50	0.21	<0.03	0.09	27.18	2.57	0.23	<0.13	101.64
apfu	**Ag**	**S**	**Fe**	**Cu**	**Bi**	**Te**	**Pb**	**Sb**	**Zn**	**As**	**Se**	
Argentotetrahedrite-(Fe)	6.08	12.42	2.00	4.27	0.01	0.00	0.01	4.10	0.08	0.04	0.00	
Argentotetrahedrite-(Fe)	5.25	12.79	1.96	4.92	0.00	0.00	0.00	4.06	0.00	0.03	0.00	
Argentotetrahedrite-(Fe)	5.11	12.70	1.88	4.93	0.02	0.03	0.03	4.11	0.16	0.03	0.00	
Argentotetrahedrite-(Fe)	4.48	12.85	1.77	5.58	0.01	0.00	0.01	4.06	0.18	0.04	0.03	
Argentotetrahedrite-(Fe)	4.08	12.91	1.82	5.99	0.02	0.03	0.01	3.89	0.23	0.02	0.00	
Argentotetrahedrite-(Fe)	3.76	12.87	1.81	6.29	0.01	0.01	0.01	3.93	0.27	0.03	0.00	
Argentotetrahedrite-(Fe)	3.40	12.98	1.78	6.52	0.03	0.02	0.01	3.97	0.25	0.04	0.00	
Argentotetrahedrite-(Fe)	3.37	12.93	1.80	6.60	0.04	0.00	0.01	3.96	0.26	0.03	0.00	
Tetrahedrite-(Fe)	2.85	12.91	1.80	6.76	0.02	0.00	0.01	3.91	0.69	0.05	0.00	

Apfu (atom per formula unit) recalculated to 29 atoms

analogous origin: Early Paleozoic S-type plutons (such as the parent rock of the Izera gneisses) may be a source of tin in the schist protolith (whether in the form of tin placers or through hydrothermal mineralization) but the present form of the deposit is a result of later tectonic deformation and is not temporally related to the intrusion itself. Romer et al. (2022) report metamorphic cassiterite in the metasedimentary Garnet Phyllite Unit from the Erzgebirge (Bockau and Aue areas in Germany). These cassiterites have U-Pb ages of 395–365 Ma, and precede 325–270 Ma granites which are the main source of tin deposits there (Romer et al., 2022). Similarly, it is likely that the tin ores in the Krobica-Gierczyn-Przecznica area were formed before the Variscan Karkonosze Granite intrusion (Michniewicz et al., 2006).

PRZECZNICA AREA

The chalcopyrite-sphalerite-rich assemblage from Przecznica is characterized by the presence of stannite (Table 4 and Fig. 3E–G), the abundant occurrence of As-phases (Table 5) and the absence of Sb-minerals that are characteristic for samples from the "Psi Grzbiet" area. Cobaltite (Fig. 3E–G) is the most abundant host of cobalt, followed by Co-bearing arsenopyrite. Arsenides containing nickel such as glaucodot and Fe-Ni diarsenides also contain Co, but were rarely observed (Table 5 and Fig. 4). Disseminated native bismuth and galena are typical accessory minerals (Fig. 3G). Chalcopyrite and sphalerite from Przecznica and the "Psi Grzbiet" area are similar in terms of chemical composition (Table 1) and match data presented by Foltyn et al. (2020). On the other hand, despite their relatively close proximity (~3 km), the sites clearly contain distinct mineral associations. Samples from Przecznica correspond to the higher temperature (250–550°C) cobaltite-arsenopyrite-glaucodot-löllingite-safflorite-bismuth parageneses of Speczik and

Wiszniewska (1984) while sulphides from the "Psi Grzbiet" area are comparable to a low temperature stage (100–250°C) with tetrahedrite (Speczik and Wiszniewska, 1984). As today's proximity between rocks forming the Stara Kamienica Schist Belt might be a result of metamorphism and tectonic shortening, it is worth to note that one simple genetic model for this polymetallic mineralization might not be sufficiently comprehensive. Quartz lenses in the "Psi Grzbiet" area may be remnants of sulphosalts-bearing quartz veins related to intrusion (such as the Izera gneiss protolith) while pyrrhotite laminations in the schist and the general Co-enrichment at Przecznica resemble a fahlband-like style of mineralization. Such ores are characterized by concordant layers or lenses with sulphidic impregnation of copper minerals and cobalt arsenides in a metamorphic sequence and are known from e.g. the Kongsberg and Modum districts in Norway.

ISOTOPIC STUDIES

SULPHUR ISOTOPES

In situ δ^{34}S measurements in sphalerite and pyrite (Fig. 5) from Przecznica are shown in Table 6. Both minerals have relatively heavy sulphur (δ^{34}S values between 8.1–9.3‰) with sphalerite isotopically slightly heavier than pyrite (9.0–9.3‰ *versus* 8.1–8.3‰).

These results are consistent with previous sulphur isotope studies on bulk samples from the Stara Kamienica Schist Belt (Berendsen et al., 1987) characterized by δ^{34}S values of +0.6‰ for pyrite from Krobica, +9 to +11.3‰ for pyrrhotite from Gierczyn and +6.6 to +8.4‰ for a pyrite-pyrrhotite mixture from Przecznica. Although different analythical methods were used to measure sulphur isotopes (bulk *versus in situ* SHRIMP *ver-*

**Representative results of EPMA chemical analyses (in wt.%) of stannite
from the Przecznica area**

Sample spot	S	Zn	Fe	In	Ag	Cu	Sn	Sum
P_AM_2A_1	29.69	1.21	12.26	<0.02	0.05	29.50	27.53	100.24
P_AM_2A_1	29.85	3.11	12.25	0.02	0.05	28.52	26.57	100.37
P_AM_2A_1	29.82	1.76	12.19	<0.02	0.02	29.32	27.59	100.70
P_AM_2A_4	29.28	3.80	12.31	0.21	0.07	27.59	26.14	99.39
P_AM_2A_5	29.56	3.67	12.34	<0.02	0.06	28.32	26.64	100.59
P_AM_2B_3	29.98	1.22	12.38	<0.02	0.03	29.29	27.62	100.52
P_AM_2B_4	30.55	2.47	11.89	<0.02	0.03	28.74	26.93	100.62
P_AM_2B_2	29.62	2.03	12.25	<0.02	0.08	28.43	26.97	99.39
AP514_1	30.10	0.93	14.13	<0.02	0.04	29.81	25.11	100.11
AP519_1	30.12	3.13	12.15	0.2	0.05	28.07	26.33	100.05

Analyses of As, Ga, Ge, Mn and Cd are not shown in the table because the results are below the detection limit of EPMA

Representative results of EPMA chemical analyses (in wt.%) of Co-bearing phases from the Przecznica area

Mineral	S	Fe	Zn	Sb	Co	Sn	Ni	Au	As	Mn	Total
Cobaltite	18.96	2.16	0.05	0.14	33.54	0.02	0.75	<0.04	44.27	<0.02	99.88
Cobaltite	19.13	2.14	<0.05	0.12	33.58	<0.02	0.98	<0.04	43.88	0.02	99.85
Cobaltite	19.02	2.11	<0.05	0.24	32.84	<0.02	1.73	<0.04	44.28	0.02	100.24
Cobaltite	18.83	2.85	0.05	2.47	30.77	<0.02	2.23	<0.04	41.91	<0.02	99.11
Cobaltite	18.39	2.98	<0.05	3.31	30.04	0.03	2.46	0.05	42.12	0.03	99.41
Cobaltite	19.00	4.25	1.14	0.59	31.59	<0.02	0.48	<0.04	43.12	0.03	100.20
Löllingite-rammelsbergite ss	0.69	18.80	<0.05	0.95	1.94	<0.02	8.22	<0.04	70.23	0.03	100.85
Glaucodot	19.40	4.97	<0.05	0.77	21.50	0.04	9.73	0.05	44.19	–	100.65
Arsenopyrite	18.92	33.52	<0.05	0.15	1.87	<0.02	0.02	<0.04	45.99	<0.02	100.47
Arsenopyrite	19.38	33.50	<0.05	0.64	2.07	<0.02	<0.02	<0.04	45.32	<0.02	100.91
Arsenopyrite	18.84	33.26	<0.05	0.13	2.18	<0.02	<0.02	<0.04	45.63	0.05	100.09
Arsenopyrite	18.74	32.93	<0.05	0.23	2.40	<0.02	0.00	<0.04	45.74	<0.02	100.04
Arsenopyrite	18.97	32.06	0.40	3.28	2.75	<0.02	0.02	0.05	43.36	0.03	100.92
Arsenopyrite	20.47	34.95	0.05	0.03	0.49	<0.02	0.00	<0.04	43.58	0.03	99.60
Arsenopyrite	20.54	33.88	<0.05	3.76	0.97	<0.02	<0.02	<0.04	40.89	–	100.04
Arsenopyrite	20.11	34.50	<0.05	1.88	1.11	<0.02	<0.02	<0.04	42.79	–	100.38
Arsenopyrite	19.23	33.85	<0.05	0.06	1.17	<0.02	<0.02	<0.04	45.99	–	100.30

– not measured; Cu, Ag, Se sought but not detected

sus in situ MC-LA-ICP-MS) these values are distinctly heavier than those reported from other polymetallic deposits and occurrences in the Karkonosze-Izera Massif. Mikulski (2010) report bulk sample $\delta^{34}S$ values of +1.71 to +4.33 for arsenopyrite, +0.07 to +3.65 for pyrite, +0.18 to +1.61 for pyrrhotite and +1.88 to +2.78 for chalcopyrite from Czarnów while Mayer et al. (2012) analysed sulphide concentrates and obtained +1.6 to +3.3‰ for pyrite from Wieściszowice, +2.7 to +4.0‰ for pyrite and pyrrhotite from Sowia Dolina, +1.1 to +1.7‰ for pyrite from Izerskie Garby, +1.3‰ for pyrite and +1.6‰ for pyrrhotite from Budniki, +1.8‰ for pyrite from Ciechanowice. *In situ* $\delta^{34}S$ values obtained using SHRIMP by Mikulski et al. (2015) are as follows: –1.97 to +2.33‰ for pyrite from Radzimowice; and –3.24 to –1.19‰ for pyrite from Leszczyniec. Sulphur isotope values

reflect the source of the sulphur, which may be magmatic in origin ($\delta^{34}S$ values typically cluster around 0 ±5‰ for magmatic-derived S), later on mixed with external sources of sulphur such as seawater (+21‰) or the crust. The isotopic composition of these ore-forming crustal fluids will depend on physical-chemical parameters such as pressure, temperature, pH and redox conditions (Ohmoto, 1972). The origin of most of these deposits (with the exception of pyrite at Wieściszowice and Leszczyniec which are thought to be related to submarine exhalative processes) is related to Variscan orogenic activity and their isotopic composition of sulphur seems to reflect the magmatic source of fluids derived from the Karkonosze Pluton (molybdenite in granite from Szklarska Poręba-Huta has a $\delta^{34}S$ value of +0.8‰; Mayer et al., 2012). The Przecznica samples
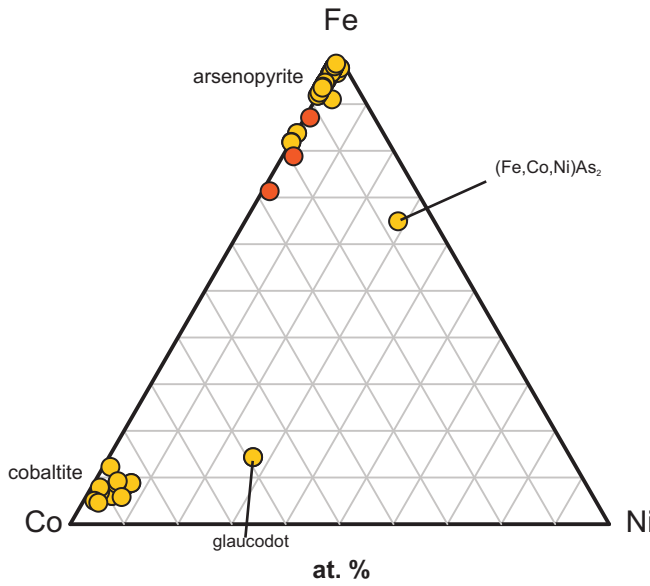
Fig. 4. Ternary diagram illustrating the relative composition regarding Co, Ni, Fe in the cation position of arsenides (atomic %) from the Przecznica and the "Psi Grzbiet" areas

Table 6

In situ **LA-ICP-MS sulphur isotopes in pyrite and sphalerite from Przecznica**

Sample spot	Mineral	δ^{34}S‰ CDT	2σ
AP513_01_1	pyrite	8.2	0.1
AP513_01_2	sphalerite	9.3	0.1
AP513_01_3	sphalerite	9.0	0.1
AP513_03_4	pyrite	8.3	0.1
AP513_03_5	pyrite	8.1	0.1
AP513_03_6	sphalerite	9.0	0.1
AP513_03_7	sphalerite	9.2	0.1

are clearly different, and while most authors suggest a magmatic provenance of solutions responsible for tin and polymetallic mineralization there (e.g., Mochnacka et al., 2015*), the isotopically heavier sulphur reported here may suggest a partial contribution of externally-derived S. An exhalative-volcanogenic origin in a submarine environment (*Lehmann and Schneider, 1981*) might not be suitable for tin ores but still can be applicable to at least part of the base metal mineralization in the Stara Kamienica Schist Belt. Early Paleozoic, stratiform, sediment-hosted Kieslager-type deposits in the*
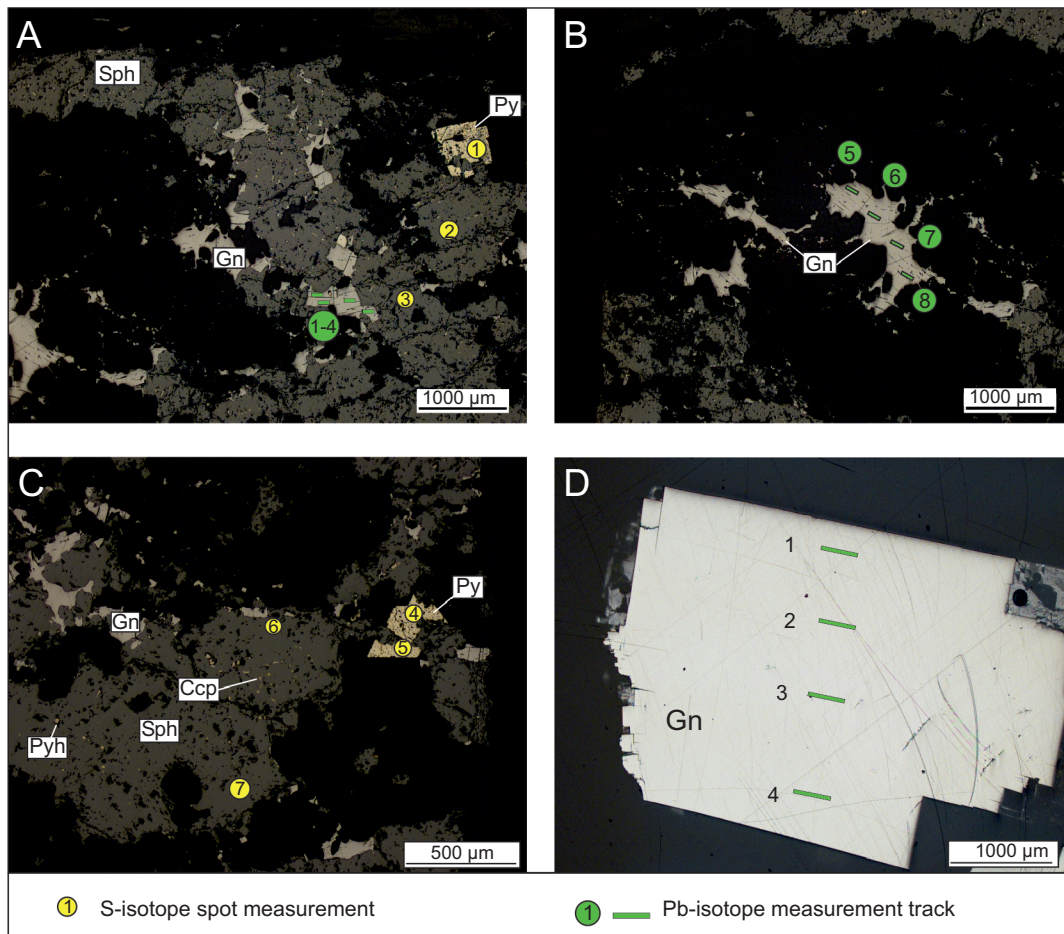
Fig. 5. Reflected light microphotographs of sulphides from Przecznica (A–C) and Strzegom (D) showing the location of spots and tracks for *in situ* sulphur and lead isotope analysis
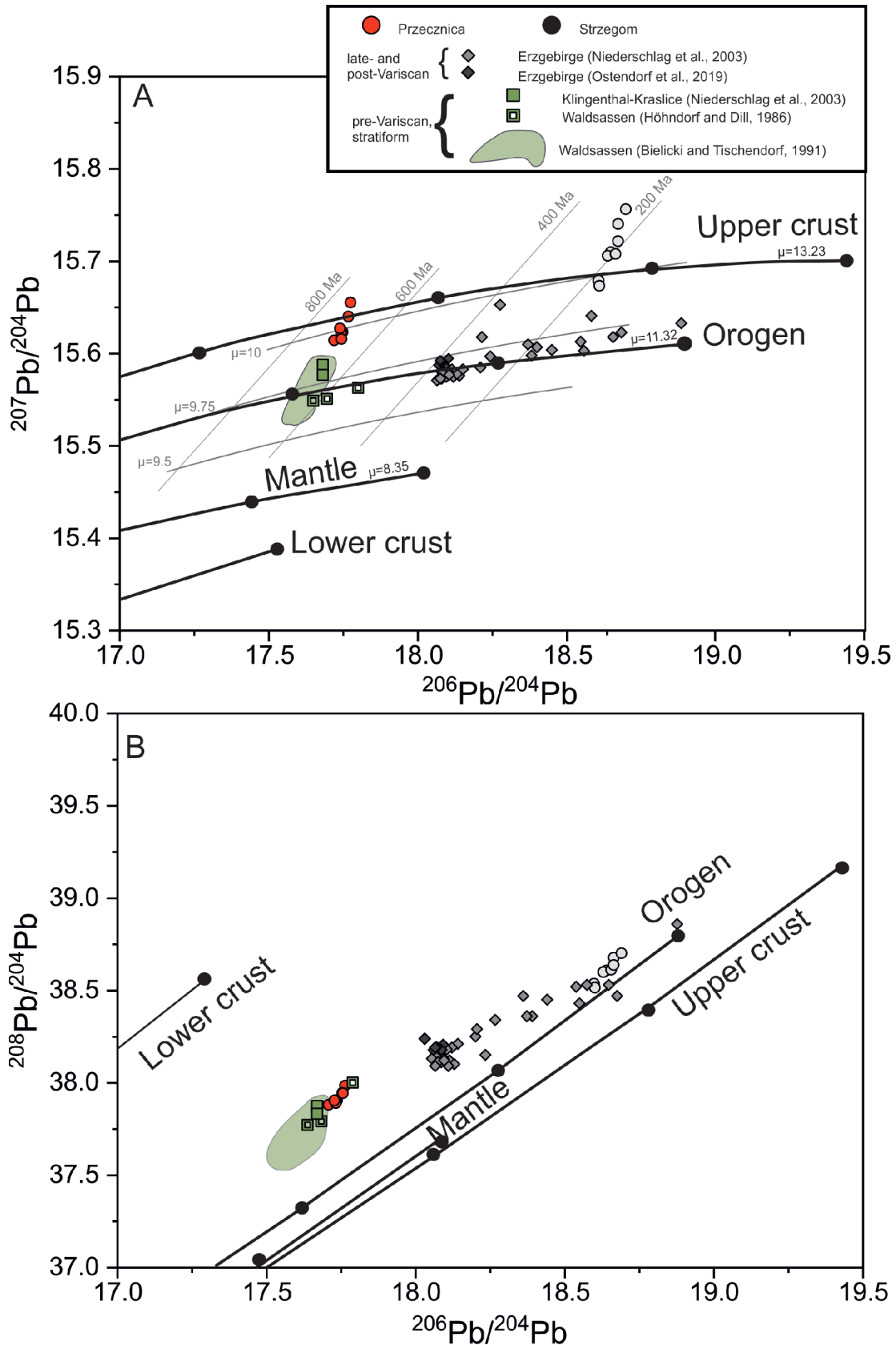
Fig. 6. Results of the *in situ* Pb-isotope analyses of galena from Przecznica and Strzegom juxtaposed with data from the NW part of the Bohemian Massif compiled from the literature

Each data point represents a single spot analysis, in contrast to bulk literature data which were acquired using TIMS (Höhndorf and Dill, 1986; Bielicki and Tischendorf, 1991; Ostendorf et al., 2019) or solution MC-ICP-MS (Niederschlag et al., 2003); **A** – distribution of data on a $^{207}Pb/^{204}Pb$ *versus* $^{206}Pb/^{204}Pb$ diagram. Pb-isotope growth curves for different reservoirs calculated according to the Zartman and Doe (1981) single stage Plumbotectonic Model 2 shown as black lines with black dots representing 0.4 Ga, while isochrons and μ-curves shown in grey are according to Stacey and Kramers (1975); **B** – distribution of data on a $^{208}Pb/^{204}Pb$ *versus* $^{206}Pb/^{204}Pb$ diagram

In situ LA-MC-ICP-MS lead isotopes in galena from Przecznica and Strzegom. Model ages calculated with PbIso (Armistead et al., 2021) using model parameters from Stacey and Kramers (1975)

Sample spot	Location	Pb^{208}/Pb^{204}	1SE	Pb^{207}/Pb^{204}	1SE	Pb^{206}/Pb^{204}	1SE	Model age [Ma]
'AP–513–Gn–1'	Przecznica	37.92390	0.02020	15.62460	0.00850	17.74470	0.01010	705
'AP–513–Gn–2'	Przecznica	37.89940	0.02570	15.61550	0.01040	17.71620	0.01280	709
'AP–513–Gn–3'	Przecznica	37.92450	0.02960	15.62400	0.01190	17.73960	0.01330	708
'AP–513–Gn–4'	Przecznica	38.00320	0.03260	15.65650	0.01350	17.77120	0.01650	744
'AP–513–Gn–5'	Przecznica	37.90870	0.03190	15.61690	0.01270	17.74050	0.01620	694
'AP–513–Gn–6'	Przecznica	37.92300	0.02430	15.62850	0.00970	17.73570	0.01160	719
'AP–513–Gn–7'	Przecznica	37.96450	0.02480	15.64040	0.01030	17.76220	0.01280	721
'AP–513–Gn–8'	Przecznica	37.96240	0.02810	15.64130	0.01190	17.76410	0.01470	721
'SP–03–1C–Gn–1'	Strzegom	38.62890	0.03120	15.71120	0.01270	18.64630	0.01470	215
'SP–03–1C–Gn–2'	Strzegom	38.61990	0.02360	15.70720	0.00960	18.63580	0.01260	215
'SP–03–1C–Gn–3'	Strzegom	38.55710	0.01690	15.68060	0.00710	18.60470	0.01040	184
'SP–03–1C–Gn–4'	Strzegom	38.53570	0.02150	15.67460	0.00910	18.60740	0.01140	169
'SP–03–1C–Gn–5'	Strzegom	38.69840	0.03980	15.74170	0.01590	18.67070	0.01970	258
'SP–03–1C–Gn–6'	Strzegom	38.72240	0.03700	15.75770	0.01580	18.69650	0.02000	271
'SP–03–1C–Gn–7'	Strzegom	38.63250	0.03130	15.70920	0.01330	18.66200	0.01560	200
'SP–03–1C–Gn–8'	Strzegom	38.65820	0.02590	15.72300	0.01110	18.67020	0.01350	221

Saxothuringian Zone such as at Waldsassen in Germany also show positive $\delta^{34}S$ values (+5 to +20‰; Dill, 1989).

LEAD ISOTOPES

In situ lead isotope ratios in galena grains collected for 18 raster lines in 3 samples are shown in Table 7.

The Pb isotope ratio variations in Przecznica samples are relatively low, typically within analytical error, while galena from Strzegom is slightly more heterogeneous (even on a scale of a single sulphide crystal). In the $^{207}Pb/^{204}Pb$ *versus* $^{206}Pb/^{204}Pb$ diagram (Fig. 6A), the population of data points from Przecznica and Strzegom form separate clusters, but both are located close to the lead isotope evolution curve of the "upper crust" reservoir (F = 13.23) defined by the Plumbotectonics Model 2 of Zartman and Doe (1981). Juxtaposition with pre-Variscan (Höhndorf and Dill, 1986; Bielicki and Tischendorf, 1991; Seifert et al., 2001; Niederschlag et al., 2003), Variscan (Niederschlag et al., 2003) and post-Variscan (Ostendorf et al., 2019) mineralization in the northwestern part of the Bohemian Massif demonstrates the resemblance of galena from Przecznica to the Early Paleozoic stratiform submarine-hydrothermal sulphide mineralization at Klingenthal-Kraslice and stratiform sulphides in Lower Paleozoic muscovite-chlorite-quartz phyllite at Waldsassen (Fig. 6). Similar mineralized horizons with tin and base metal sulphides has been reported in metasedimentary rocks of the Preßnitz Group north of Freiberg in Germany (Lehmann and Schneider, 1981; Járóka and Seifert, 2015) but available Pb isotope data from this location refer to the Mesozoic Pb-Ba vein and not to the mica schist-hosted mineralization (Bielicki and Tischendorf, 1991). These results support the idea of a pre-metamorphic origin of mineralization (e.g., Jaskólski, 1948; Cook and Dudek, 1994; Michniewicz et al., 2006; Foltyn et al., 2020) rather than a post-metamorphic genesis related to the Karkonosze granite intrusion (e.g., Jaskólski and Mochnacka, 1959; Speczik and Wiszniewska, 1984; Mochnacka et al., 2015).

Pb-Pb ages of galena from Przecznica were calculated with PbIso (Armistead et al., 2021) using model parameters from Stacey and Kramers (1975) and gave Neoproterozoic model ages between 694 and 721 Ma (Table 6 and Fig. 6A), older than the established geochronology of this area (620–500 Ma). The age of the mica schists hosting the mineralization is uncertain; they could represent the Neoproterozoic country rock of the ~500 Ma granite protolith of the orthogneisses (Mazur et al., 2006) or the volcanogenic-sedimentary succession deposited contemporaneously with the Early Paleozoic intrusions (Oberc-Dziedzic et al., 2010). A volcanogenic intercalation in the Złotniki Lubańskie schists was dated to 560 Ma and contained zircons that grew at 620 Ma and 600–580 Ma (Żelaźniewicz et al., 2009) indicating they could represent a metamorphosed equivalent of the 570 Ma old Lusatian greywackes (Linnemann et al., 2000; Oberc-Dziedzic et al., 2009; Żelaźniewicz et al., 2009). Multiple metamorphic events associated with the Cadomian and later Variscan orogenies might have caused the circulation of Pb-rich fluids carrying the old radiogenic signature and this may be one of the reasons for the apparently older ages of the galena.

Pb-Pb ages for sample from Strzegom (data scattered between 271 and 169 Ma) are younger than the established age of granite intrusions forming the Strzegom-Sobótka Massif (305–295 Ma, Turniak et al., 2014). Re-Os ages of molybdenite from the Strzegom-Sobótka Massif in general fall in the range 309 ±1 to 296 ±2 Ma (Mikulski and Stein, 2012) but molybdenite found in a two mica-granite from Siedlimowice gave an age of 257 ±1 Ma, which was interpreted as an indicator of tectonic reactivation and remobilization of hydrothermal fluids in the Late Permian (Mikulski and Stein, 2012). The Pb isotopic character is related not solely to the age but also to petrogenesis and crustal contamination might play a role e.g., Halla (2018). Domańska-Siuda et al. (2019) show that the Strzegom-Sobótka Pluton exhibits ambiguous isotopic and geochemical signatures and represents a multi-component system with melts derived from heterogeneous crustal domains. Remobilization of hydrothermal fluids, crustal contamination and the fact that analysed

galena crystals were found in a pegmatite druse in granite, representing a magmatic–hydrothermal stage enriched in uranium relative to the granitic melt, could all affect the Pb-isotope signature in the Strzegom sample. Further studies of Pb-Pb isotopes in the Sudetes Mountains are needed to better understand Pb isotopic reservoirs in the Bohemian Massif and explain discrepancies between Pb-Pb model ages reported here and established geochronological data.

Both Przecznica and Strzegom plot very close to or above the upper crust Pb average evolution curve, especially when compared with the data for mineralization in the NW part of the Bohemian Massif compiled from the literature (Fig. 6). Although they were obtained with different methods (TIMS, solution MC-ICP-MS and *in situ* LA-MC-ICP-MS), the alignment of Waldsassen, Klingenthal-Kraslice and Przecznica data along a noticeable trend (Fig. 6A) could potentially represent a mixing line between mantle and a crustal Pb reservoir although more data are necessary to confirm this.

CONCLUSIONS

• Sulphide mineralization in the Stara Kamienica Schist Belt exhibit diverse mineralogy including rare Te-canfieldite (reported only in a handful of localities worldwide), "freibergite--(Fe)", garavellite, hedleyite, joseite-A, ullmannite, native Bi, galena, Bi-rich jamesonite, cobaltite, stannite, arsenopyrite and glaucodote. However, they occur only as accessory minerals and their quantities are too low to be of economic importance

• Despite relatively the small distance (3 km) between the areas studied, they show distinct geochemical and mineralogical differences. Samples collected in the "Psi Grzbiet" area are very similar to those reported from the Jialong Cu-Sn deposit in China related to a shear zone and are characterized by the presence of Ag, Ni, Sb, and Te minerals with very little arsenopyrite. The mineralogy of the Przecznica area is characterized by an abundance of As phases represented mainly by cobaltite and arsenopyrite with a simultaneous lack of Sb minerals.

• S isotope values of Przecznica samples, although determined with a different method (*in situ* MC-LA-ICP-MS rather than bulk samples), are heavier than in most deposits related to the Karkonosze Granite intrusion, suggesting a different origin for or an additional source of sulphur.

• The Pb isotope signature in galena from Przecznica resembles Early Paleozoic pre-Variscan mineralization rather than Variscan mineralization, supporting the inference that the origin of the galena-sphalerite-pyrite mineralization is pre-metamorphic and therefore the post-metamorphic Karkonosze Pluton cannot be its source.

REFERENCES

Armistead, S.E., Eglington, B.M., Pehrsson, S.J., 2021. PbIso: an R package and web app for calculating and plotting Pb isotope data. EarthArXiv. https//doi.org/10.31223/X56G84

Berendsen, P., Speczik, S., Wiszniewska, J., 1987. Sulphide geochemical studies of the stratiform tin deposits in the Stara Kamienica Chain (SW Poland). Archiwum Mineralogiczne, **42**: 31–42.

Bielicki, K.H., Tischendorf, G., 1991. Lead isotope and Pb-Pb model age determinations of ores from Central Europe and their metallogenetic interpretation. Contributions to Mineralogy and Petrology, **106**: 440–461. https://doi.org/10.1007/BF00321987

Borkowska, M., Hameurt, J., Vidal, P., 1980. Origin and age of Izera gneisses and Rumburk granites in the Western Sudetes. Acta Geologica Polonica, **30**: 121–146.

Chen, L., Wang, Z., Yan, Z., Gong, J., Ma, S., 2018. Zircon and cassiterite U-Pb ages, petrogeochemistry and metallogenesis of Sn deposits in the Sibao area, northern Guangxi: constraints on the Neoproterozoic granitic magmatism and related Sn mineralization in the western Jiangnan Orogen, South China. Mineralogy and Petrology, **112**: 437–463. https://doi.org/10.1007/s00710–018–0554–2

Cook, N.J., Dudek, K., 1994. Mineral chemistry and metamorphism of garnet-chlorite-mica schists associated with cassiterite-sulphide-mineralisation from the Kamienica Range, Izera Mountains, SW Poland. Chemie der Erde, **54**: 1–32.

Dill, H. G., 1989. Metallogenetic and geodynamic evolution in the Central European Variscides – a pre-well site study for the German Continental Deep Drilling Programme. Ore Geology Reviews, **4**: 279–304. https://doi.org/10.1016/0169-1368(89)90007-3.

Domańska-Siuda, J., Słaby, E., Szuszkiewicz, A., 2019. Ambiguous isotopic and geochemical signatures resulting from limited melt interactions in a seemingly composite pluton: a case study from the Strzegom–Sobótka Massif (Sudetes, Poland). International Journal of Earth Sciences, **108**: 931–962. https://doi.org/10.1007/s00531-019-01687-w

Foltyn, K., Erlandsson, V.B., Kozub-Budzyń, G.A., Melcher, F., Piestrzyński, A., 2020. Indium in polymetallic mineralisation at the Gierczyn mine, Karkonosze-Izera Massif, Poland: results of EPMA and LA-ICP-MS investigations. Geological Quarterly, **64** (1): 74–85. https//doi.org/10.7306/gq.1516

Gilbert, S.E., Danyushevsky, L.V., Rodermann, T., Shimizu, A., Gurenko, A., Meffre, S., Thomas, H., Large, R.R., Death, D., 2014. Optimisation of laser parameters for the analysis of sulphur isotopes in sulphide minerals by laser ablation ICP-MS. Journal of Analytical Atomic Spectrometry, **29**: 1042–1051. https://doi.org/10.1039/C4JA00011K

Halla, J., 2018. Pb isotopes – a multi-function tool for assessing tectonothermal events and crust-mantle recycling at late Archaean convergent margins. Lithos, **320**: 207–221. https://doi.org/10.1016/j.lithos.2018.08.031

Höhndorf, A., Dill, H., 1986. Lead isotope studies of strata-bound, vein-type, and unconformity-related Pb, Sb, and Bi ore mineralizations from the western edge of the Bohemian Massif (FR Germany). Mineralium Deposita, **21**: 329–336. https://doi.org/10.1007/BF00204353

Járóka, T., Seifert, T., 2015. Characterization of the hydrothermal Sn–polymetallic "Felsitzone" mineralization of Großschirma, Freiberg mining district, Saxony, Germany. Mineral resources in

a sustainable world. 13th SGA Biennial Meeting, 24–27 August 2015, Nancy, France, 2: 773–776.

Jaskólski, S., 1948. Tin ore deposit in Gerbichy (Gieren) in Lower Silesia (preliminary report) (in Polish with English summary). Biuletyn Państwowego Instytutu Geologicznego, 42: 1–22.

Jaskólski, S., Mochnacka, K., 1959. Tin deposits at Gierczyn in Isera Mountains, Lower Silesia an attempt of elucidation their origin. Archiwum Mineralogiczne, 22: 17–106.

Kołodziejczyk, J., Pršek, J., Voudouris, P.C., Melfos, V., 2017. Bi-sulphotellurides associated with Pb-Bi-(Sb ±Ag, Cu, Fe) sulphosalts: an example from the Stan Terg deposit in Kosovo. Geologica Carpathica, 68: 366–381.
https://doi.org/10.1515/geoca-2017-0025

Lehmann, B., Schneider, H.J., 1981. Strata-bound tin deposits. In: Handbook of Strata–bound and Stratiform Ore Deposits (eds. K.H. Wolf): 743–771. Elsevier.

Linnemann, U., Gehmlich, M., Tichomirowa, M., Buschmann, B., Nasdala, L., Jonas, P., Lützner, H., Bombach, K., 2000. From Cadomian subduction to Early Palaeozoic rifting: the evolution of Saxo-Thuringia at the margin of Gondwana in the light of single zircon geochronology and basin development (Central European Variscides, Germany). Geological Society Special Publications, 179: 131–153.
https://doi.org/10.1144/GSL.SP.2000.179.01.10

Liu, J., Chen, W., Liu, Q., 2018. Sb-Bi alloys and Ag-Cu-Pb-Sb-Bi sulphosalts in the Jialong Cu-Sn deposit in North Guangxi, South China. Minerals, 8: 26.
https://doi.org/10.3390/min8010026

Madziarz, M., Sztuk, H., 2008. Kopalnia "Gierczyn" – zapomniany epizod w historii górnictwa rud Ziem Zachodnich (in Polish). Dzieje Górnictwa - element europejskiego dziedzictwa kultury, (eds. P.P. Zagożdżon and M. Madziarz): 195–212, Oficyna Wydawnicza Politechniki Wrocławskiej, Wrocław.

Małek, R., Mikulski, S.Z., 2021. A rare indium-bearing mineral (Zn-In-Cu-Fe sulphide) from the Stara Kamienica Schist Belt (Sudetes, SW Poland). Geological Quarterly, 65 (1): 7.
https://doi.org/10.7306/gq.1572

Mayer, W., Jędrysek, M.O., Górka, M., Drzewicki, W., Mochnacka, K., Pieczka, A., 2012. Preliminary results of sulphur isotope studies on sulphides from selected ore deposits and occurrences in the Karkonosze-Izera Massif (the Sudety Mts., Poland). Mineralogia, 43: 213–222.

Mazur, S., Aleksandrowski, P., 2001. The Tepla (?)/Saxothuringian suture in the Karkonosze-Izera Massif, western Sudetes, Central European Variscides. International Journal of Earth Sciences, 90: 341–360. https://doi.org/10.1007/s005310000146

Mazur, S., Kryza, R., 1996. Superimposed compressional and extensional tectonics in the Karkonosze-Izera Block, NE Bohemian Massif. In: Basement Tectonics 11 Europe and Other Regions (eds. O. Oncken and C. Janssen): 51–66. Springer, Dordrecht.

Mazur, S., Aleksandrowski, P., Kryza, R., Oberc-Dziedzic, T., 2006. The Variscan orogen in Poland. Geological Quarterly, 50 (1): 89–118.

Mazur, S., Aleksandrowski, P., Szczepański, J., 2010. Outline structure and tectonic evolution of the Variscan Sudetes (in Polish with English summary). Przegląd Geologiczny, 58: 133–145.

Mederski, S., Pršek, J., Dimitrova, D., Hyseni, B., 2021. A combined EPMA and LA-ICP-MS investigation on Bi-Cu-Au mineralization from the Kizhnica Ore Field (Vardar Zone, Kosovo). Minerals, 11: 1223. https://doi.org/10.3390/min11111223

Michniewicz, M., Bobiński, W., Siemiątkowski, J., 2006. The mineralization in the middle part of the Stara Kamienica Schist Belt (Western Sudetes) (in Polish with English summary). Prace Państwowego Instytutu Geologicznego, 185: 5–136.

Mikulski, S.Z., 2007. Metal ore potential of the parent magma of granite – the Karkonosze massif example. Granitoids in Poland. Archivum Mineralogiae Monograph 1: 123–145.

Mikulski, S.Z., 2010. The characteristic and genesis of the gold-bearing arsenic polymetallic mineralization in the Czarnów deposit (Western Sudetes) (in Polish with English summary). Biuletyn Państwowego Instytutu Geologicznego, 439: 303–320.

Mikulski, S.Z., Małek, R., 2020. Rudy cyny (tin ores) (in Polish). In: Bilans perspektywicznych zasobów kopalin Polski wg stanu na 31.12.2018 r. (eds. K. Szamałek, M. Szuflicki and W. Mizerski): 162–167. PIG-PIB, Warszawa.

Mikulski, S.Z., Stein, H.J., 2012. The age of molybdenites in Poland in the light of Re-Os isotopic studies (in Polish with English summary). Biuletyn Państwowego Instytutu Geologicznego, 452: 199–216.

Mikulski, S.Z., Krzemińska, E., Czupyt, Z., Williams, I.S., 2015. Sulphur isotope measurements of sulphide minerals from the polymetallic ore deposits in the Sudetes, using the SHRIMP IIe/MC ion microprobe (in Polish with English summary). Biuletyn Państwowego Instytutu Geologicznego, 464: 61–78.

Mikulski, S.Z., Williams, I.S., Stein, H.J., Wierchowiec, J., 2020. Zircon U-Pb dating of magmatism and mineralizing hydrothermal activity in the Variscan Karkonosze Massif and its eastern metamorphic cover (SW Poland). Minerals, 10: 787.
https://doi.org/10.3390/min10090787

Mochnacka, K., Oberc-Dziedzic, T., Mayer, W., Pieczka, A., 2015. Ore mineralization related to geological evolution of the Karkonosze-Izera Massif (the Sudetes, Poland) – towards a model. Ore Geology Reviews, 64: 215–238.
https://doi.org/10.1016/j.oregeorev.2014.07.001

Molnár, F., O'Brien, H., Lahaye, Y., Käpyaho, A., Sorjonen-Ward, P., Hyodo, H., Sakellaris, G., 2016. Signatures of multiple mineralization processes in the Archean orogenic gold deposit of the Pampalo mine, Hattu schist belt, eastern Finland. Economic Geology, 111: 1659–1703.
https://doi.org/10.2113/econgeo.111.7.1659

Molnár, F., Middleton, A., Stein, H., O'Brien, H., Lahaye, Y., Huhma, H., Johanson, B., 2018. Repeated syn- and post-orogenic gold mineralization events between 1.92 and 1.76 Ga along the Kiistala Shear Zone in the Central Lapland Greenstone Belt, northern Finland. Ore Geology Reviews, 101: 936–959. https://doi.org/10.1016/j.oregeorev.2018.08.015

Müller, W., Shelley M., Miller, P., Broude, S., 2009. Initial performance metrics of a new custom–designed ArF excimer LA-ICPMS system coupled to a two-volume laser-ablation cell. Journal of Analytical Atomic Spectrometry, 24: 209–214.
https://doi.org/10.1039/B805995K

Niederschlag, E., Pernicka, E., Seifert, T., Bartelheim, M., 2003. The determination of lead isotope ratios by multiple collector ICP MS: a case study of Early Bronze Age artefacts and their possible relation with ore deposits of the Erzgebirge. Archaeometry, 45: 61–100.
https://doi.org/10.1111/1475-4754.00097

Oberc-Dziedzic, T., Pin, C., Kryza, R., 2005. Early Palaeozoic crustal melting in an extensional setting: petrological and Sm-Nd evidence from the Izera granite-gneisses, Polish Sudetes. International Journal of Earth Sciences, 94: 354–368.
https://doi.org/10.1007/s00531-005-0507-y

Oberc-Dziedzic, T., Kryza, R., Pin, C., Mochnacka, K., Larionov, A., 2009. The orthogneiss and schist complex of the Karkonosze-Izera massif (Sudetes, SW Poland): U-Pb SHRIMP zircon ages, Nd-isotope systematics and protoliths. Geologia Sudetica, 41: 3–24.

Oberc-Dziedzic, T., Kryza, R., Mochnacka, K., Larionov, A., 2010. Ordovician passive continental margin magmatism in the Central-European Variscides: U-Pb zircon data from the SE part of the Karkonosze-Izera Massif, Sudetes, SW Poland. International Journal of Earth Sciences, 99: 27–46.
https://doi.org/10.1007/s00531-008-0382-4

Ohmoto, H., 1972. Systematics of sulphur and carbon isotopes in hydrothermal ore deposits. Economic Geology, 67: 551–578, https://doi.org/10.2113/gsecongeo.67.5.551

Ostendorf, J., Henjes-Kunst, F., Seifert, T., Gutzmer, J., 2019. Age and genesis of polymetallic veins in the Freiberg district, Erzgebirge, Germany: constraints from radiogenic isotopes. Mineralium Deposita, 54: 217–236.
https://doi.org/10.1007/s00126-018-0841-1

Piestrzyński, A., Mochnacka, K., 2003. Discussion on the sulphide mineralization related to the tin-bearing zones of the Kamienica

schists belt (Western Sudety Mountains, SW Poland) (in Polish with English summary). In: The Western Sudetes: From Vendian to Quaternary (eds. W. Ciężkowski, J. Wojewoda and A. Żelaźniewicz): 169–182. WIND, Wrocław

Pršek, J., Ozdín, D., Sejkora, J., 2008. Eclarite and associated Bi sulfosalts from the Brezno–Hviezda occurrence (Nízke Tatry Mts, Slovak Republic). Neues Jahrbuch für Mineralogie Abhandlungen, **185**: 117.
https://doi.org/10.1127/0077-7757/2008/0112

Romer, R.L., Kroner, U., Schmidt, C., Legler, C., 2022. Mobilization of tin during continental subduction-accretion processes. Geology, **50**: 1361–1365. https://doi.org/10.1130/G50466.1

Seifert, T., Niederschlag, E., Pernicka, E., Fiedler, F., 2001. Lead isotope pilot study from ore deposits in the Erzgebirge, Germany, and surrounded areas by multiple-collector inductively coupled plasma mass spectrometry (MC-ICP-MS). In: Mineral Deposits at the Beginning of the 21st Century (ed. A. Piestrzyński): 1095–1098. CRC Press.

Speczik, S., Wiszniewska, J., 1984. Some comments about stratiform tin deposits in the Stara Kamienica Chain (southwestern Poland). Mineralium Deposita, **19**: 171–175.
https://doi.org/10.1007/BF00199781

Stacey, J.T., Kramers, J.D., 1975. Approximation of terrestrial lead isotope evolution by a two-stage model. Earth and Planetary Science Letters, **26**: 207–221.
https://doi.org/10.1016/0012-821X(75)90088-6

Stevenson, R.K., Martin, R.F., 1986. Implications of the presence of amazonite in the Broken Hill and Geco metamorphosed sulphide deposits. Canadian Mineralogist, **24**: 729–745.

Townsend, A.T., Yub, Z., McGoldrick, P., Hutton, J.A., 1998. Precise lead isotope ratios in Australian galena samples by high resolution inductively coupled plasma mass spectrometry. Journal of Analytical Atomic Spectrometry, **13**: 809–813.
https://doi.org/10.1039/A801397G

Turniak, K., Mazur, S., Domańska-Siuda, J., Szuszkiewicz, A., 2014. SHRIMP U-Pb zircon dating for granitoids from the Strzegom-Sobótka Massif, SW Poland: constraints on the initial time of Permo-Mesozoic lithosphere thinning beneath Central Europe. Lithos, **208**: 415–429.
https://doi.org/10.1016/j.lithos.2014.09.031

Verhoef, E.V., Dijkema, G.P., Reuter, M.A., 2004. Process knowledge, system dynamics, and metal ecology. Journal of Industrial Ecology, **8**: 23–43. https://doi.org/10.1162/1088198041269382

Yue, Z.H., Bai, L.A., Hu, R.G., Wu, J., Dai, Y., Zhou, S.Y., Feng, Z.H., Xu, C., Zhao Z.X., Liu, X.J., 2022. Caledonian tin mineralization in the Jiuwandashan area, Northern Guangxi, South China. Minerals, **12**: 843. https://doi.org/10.3390/min12070843.

Zartman, R.E., Doe, B.R., 1981. Plumbotectonics – the model. Tectonophysics, **75**: 135–162.
https://doi.org/10.1016/0040-1951(81)90213-4

Żelaźniewicz, A., Nowak, I., Achramowicz, S., Czapliński, W., Ciężkowski, A., Wojewoda, J., 2003. The northern part of the Izera-Karkonosze Block: a passive margin of the Saxothuringian terrane (in Polish with English summary). In: The Western Sudetes: From Vendian to Quaternary (eds. W. Ciężkowski, J. Wojewoda and A. Żelaźniewicz): 17–32. WIND, Wrocław.

Żelaźniewicz, A., Fanning, C.M., Achramowicz, S., 2009. Refining the granite, gneiss and schist interrelationships within the Lusatian-Izera Massif, West Sudetes, using SHRIMP U-Pb zircon analyses and new geologic data. Geologia Sudetica, **41**: 67–84.